Noniterative Density Functional Response Approach: Application to Nonlinear Optical Properties of *p*-Nitroaniline and Its Methyl-Substituted Derivatives

K. B. Sophy,† Sapana V. Shedge, and Sourav Pal*

Theory Group, Physical Chemistry Division, National Chemical Laboratory, Pune 411 008, India

Received: July 14, 2008; Revised Manuscript Received: August 19, 2008

We report the effect of substitution, position of the substituent, and the symmetry on the nonlinear optical properties of *p*-nitroanline (PNA) and its derivatives using our implementation of the noniterative approximation of couple-perturbed Kohn−Sham (CPKS) equation in the deMon2k. Dipole moment, static polarizability, and first hyperpolarizability of these π-conjugated donor−acceptor organic derivatives of PNA and its methyl-substituted analogs are calculated using our method at different exchange correlation functionals, namely, BP86, BPW91, and BLYP, using 6-31++G** basis set. A comparison of results obtained by our method with those obtained by MP2 (finite-field perturbation) method is presented in this paper. The effect of optical gap on charge transfer and subsequently on polarizabilities has been illustrated.

Introduction

The area of nonlinear optics (NLO) continues to be in the limelight since past few decades. There has been tremendous advancement in the field of NLO materials and the experimental techniques available to study them. Progress in the development of many such technologically important processes in areas of optical information processing, telecommunications, integrated optics, optical computers, laser technology, etc., is based on understanding of molecular properties of the constituent materials. A change in the environment of a molecule has an effect on its structural and physical properties. The effect of a weak external perturbation on the electronic distribution of the molecule is thus reflected in its response properties. Response electric properties, in particular, have been studied for a wide variety of atoms and molecules in the past using different approaches. Materials with high second-order responses are considered important for NLO applications. Organic molecules with delocalized π electrons have attracted a lot of attention as they exhibit particularly large nonlinear responses.[1] The microscopic structure−property relationship for such molecules may lead to discovery of improved NLO characteristics in materials, thus, facilitating the design of new molecules for potential NLO applications.[2] This could be done through study of response electric properties, namely, polarizability and hyperpolarizability, of the molecules using computational methods.

Electron-correlation effects play a crucial role in the determination of these properties. NLO properties of a variety of push−pull phenylenes have been studied extensively.[3,4] The sensitivity of the NLO properties to the conjugation length, donor and acceptor substitutions, and effects due to symmetry in the molecule are well-known.[5] Over the period, *p*-nitroaniline (PNA) has been identified as a prototype system to understand the large nonlinear responses exhibited due to the presence of donor−acceptor moieties which lead to charge transfer in the PNA molecule. There are number of studies available for the PNA molecule.[6−13] Bulat et al.[14] studied the PNA molecule as well as the effect of chain length on electric properties of aliphatic push−pull compounds at different levels of theory and discussed the effect of electron correlation on the calculations. Determination of first and second order polarizability, in particular, plays an important role in understanding the response of molecule to an external weak electric perturbation. Electric response properties[15−22] has been studied extensively using *ab initio* methods[22−24] as well as density functional theory (DFT) for both atoms and molecules. DFT among other theoretical methods has been used to study electric properties of such materials. The Hartree−Fock theory like computational scaling, while accounting for electron-correlation effects, makes DFT an obvious choice for large scale computations.

The present work reports the static response electric properties, namely, dipole moment, polarizability, and first hyperpolarizability for PNA and its methyl-substituted derivatives[25] obtained using our noniterative coupled-perturbed Kohn−Sham (CPKS) approach, proposed earlier.[25−29] The structures of all the molecules used for the calculations have been given in Figure 1. A short label has been given for each of the molecules below their complete names in Figure 1 for easy reference during the discussion of results. The effect of substitution on polarizabilities as well as on dipole moment has been discussed in detail. We have also studied how the optical gap affects charge transfer and subsequently the polarizability values. Comparison of our results has been done with MP2 values reported by Davis et al.[8] We give a brief description of our method and the computational details of the calculation in the following section.

Method

The CPKS method is useful for obtaining the response of the electron density to an external perturbation which, in turn, can be used to evaluate the response electric properties of molecules. The CPKS matrix equation for a static, homogeneous electric field perturbation is the derivative of the Kohn−Sham (KS) matrix equation with respect to the electric field and can be given as

$$H'C^{(0)} + HC' = S'C^{(0)}E + SC'E + SC^{(0)}E' \qquad (1)$$

where, the primes denote the derivative with respect to electric field perturbation and the superscript (0) denotes an unperturbed

* To whom correspondence should be addressed. E-mail: s.pal@ncl.res.in.
† Present address: Division of Physics & Applied Physics, School of Physical and Mathematical Sciences, Nanyang Technological University, Singapore 637371 Singapore.

10.1021/jp806204q CCC: $40.75
Published on Web 10/10/2008

calculation. The derivative or response coefficient matrix, C', in eq 1, is written in terms of a new matrix U', and the unperturbed coefficient matrix as

$$C' = C^{(0)}U' \tag{2}$$

Thus, the CPKS matrix equation (eq 1), simplifies to[30]

$$U'_{ia} = \frac{\sum_{\mu,\nu} C^{\dagger}_{\mu i} H'_{\mu\nu} C_{va}}{(\varepsilon_i - \varepsilon_a)} \tag{3}$$

where, index i spans the occupied molecular orbitals (MO), index a spans the virtual MOs, μ and ν are the indices for the atomic orbitals (AO), and C and ε_i are the coefficient matrix and eigenvalues of the Kohn−Sham matrix, respectively, for the unperturbed DFT calculations. Matrix H' is the derivative of the field-dependent KS operator matrix in the AO basis and constitutes the explicit derivative of the 2-electron potential terms and the dipole moment operator matrix. For closed-shell cases, the occupied virtual block of the U' matrix is negative to the virtual-occupied block and the remaining elements of the matrix are zero. Matrix U' is the solution of the CPKS equations which gives the C' matrix from eq 2. The C' matrix along with the unperturbed coefficient matrix gives the derivative or response density matrix, P'

$$P'_{\mu\nu} = \sum_i (C'_{\mu i} C_{\nu i} + C'_{\nu i} C_{\mu i}) \tag{4}$$

Further, the P' matrix, which is the first-order response of the electron density to the external electric field perturbation obtained using a variational method,[31] could give the response electric properties or derivatives of energy[32,33] with respect to electric field, up to third order by the $(2n + 1)$ rule for energy derivatives.[34] In principle, due to the implicit dependence of the H' on C' matrix, the CPKS equation requires to be solved iteratively for each of the x, y, and z components of the dipole moment operator matrix in the H'. The first step to this method is the programming of the complicated algebraic equations involving the 2-electron terms in the H' matrix for the different exchange-correlation functionals available, which is a huge task. Second, the solution of the completely analytic CPKS method (eq 3) becomes highly time-consuming due to the iterative nature which requires the complicated H' matrix construction using the C' matrix of an earlier iteration, for each iteration, until self-consistency is reached.

We have introduced a simplification to the analytic CPKS matrix equation, thereby transforming it, to give a single-step solution.[25−29] This requires use of the H' constructed using a finite-field method in the CPKS equation (eq 3) to obtain a one-step solution. For this, the field-dependent KS operator matrix, $H(\mathrm{F})$, is obtained for different electric field perturbations close

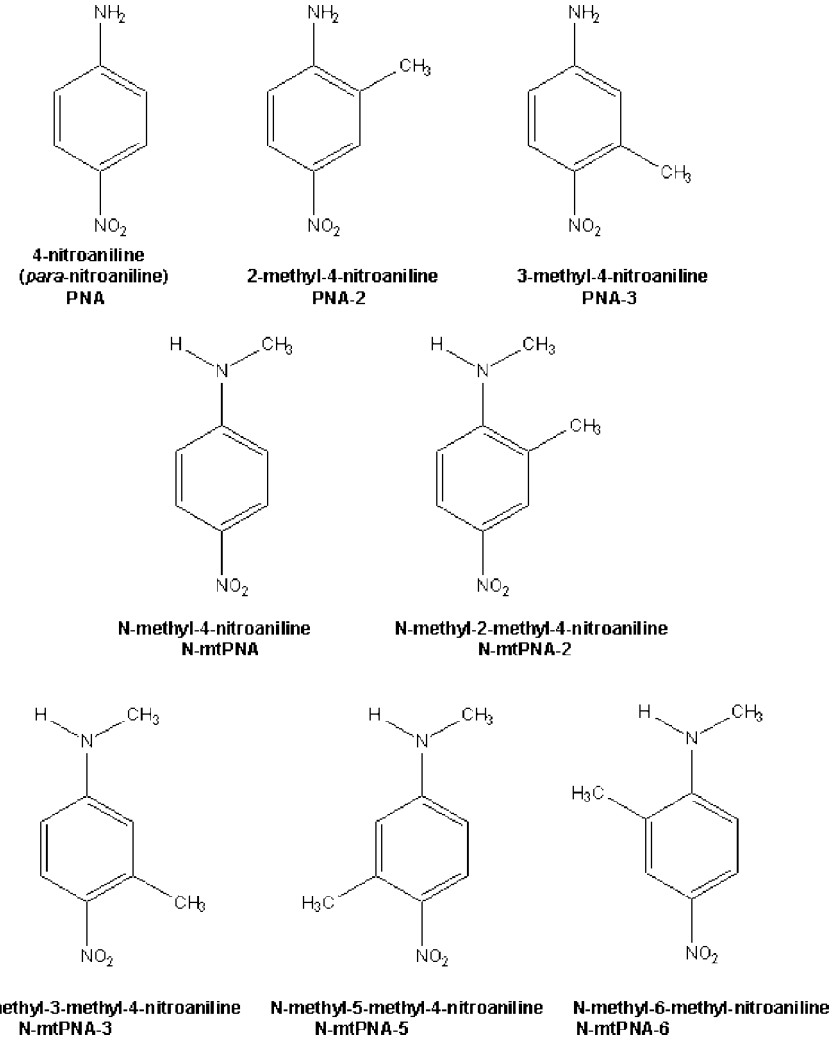

Figure 1. Structures of PNA and its methyl-substituted derivatives along with their abbreviated names used in the present work.

to zero (in the x, y, and z directions), and these are used in the three-point formula for first derivatives to obtain the H' matrix (x, y, and z components). Plugging in these three components of the newly constructed H' along with the coefficient matrix and the eigenvalues from the unperturbed KS calculation, in eq 3, gives three CPKS matrix equations, whose solutions are thus obtained in a single step. We thus get the response density matrix through our method, which completely circumvents the complicated construction of the H' matrix thus saving computational time and effort. This implementation could prove highly useful for applications involving large molecules using large basis sets.

As described earlier, we make use of the $(2n + 1)$ rule[34] for higher-energy derivatives. Thus, the first-order response in the form of derivative density matrix obtained from the solution of the CPKS matrix equation is used to obtain the second-order as well as the third-order response properties, namely, dipole polarizability and the first hyperpolarizability. The dipole polarizability is obtained as

$$\alpha = \text{trace}(H' P') \tag{5}$$

The third derivative of energy, i.e., the dipole first hyperpolarizability is obtained as

$$\beta = \text{trace}(H' P' P') \tag{6}$$

where H' is the derivative KS operator matrix in the AO basis. The dipole moment is calculated as

$$\mu = \sqrt{\mu_x^2 + \mu_y^2 + \mu_z^2} \tag{7}$$

Mean and anisotropic polarizability and mean first hyperpolarizabilities values are obtained using the respective tensor components. The mean polarizability is calculated from the poarizability components as

$$\bar{\alpha} = \frac{1}{3}(\alpha_{xx} + \alpha_{yy} + \alpha_{zz}) \tag{8}$$

and, the polarizability anisotropy is obtained as

$$|\bar{\alpha}| = \frac{3tr\alpha^2 - (tr\alpha)^2}{2}(\text{general axis}) \tag{9}$$

$$= \frac{1}{2}[(\alpha_{xx} - \alpha_{yy})^2 + (\alpha_{xx} - \alpha_{zz})^2 + (\alpha_{yy} - \alpha_{zz})^2(\text{principal axis}) \tag{10}$$

The orientationally averaged first hyperpolarizability are obtained as

$$\beta_i = \frac{1}{3}\sum_k \beta_{ikk} \tag{11}$$

whereas, the average static first hyperpolarizability is obtained as

$$\beta = \sqrt{\beta_x^2 + \beta_y^2 + \beta_z^2} \tag{12}$$

Computational Details

We have used the geometries optimized at the MP2 level using the 6-31++G** basis previously reported.[8] We report the dipole moments, dipole polarizability, and first hyperpolarizability calculation using the finite-field perturbation method (MP2) for the set of chosen molecules. The structures of molecules used in the present work are given in Figure 1. Throughout our calculations the molecule is in the xy plane with the x axis being along the direction of the maximal extension with the amine group on the positive side of the x axis and the z axis perpendicular to the molecular plane. We have done the response property calculations at the DFT level of theory for different nonlocal exchange-correlation functionals using the 6-31++G** basis. The calculations are done using our implementation of the approximate CPKS method in the version 1.7 of deMon2k.[35] The A2 auxiliary basis was used for fitting the electron density, whereas the exchange correlation potential has been evaluated using the orbital basis, which is the case for the VXCTYPE BASIS option in the deMon2k. The working equations used for α and β calculations along with a brief description of our method has been done in our previous papers.[25−29] We have carried out the calculations using the BP86,[36,37] BPW91,[36,38] and BLYP[36,39] nonlocal DFT functionals. The calculations have been done using the electric field value intervals of 0.001 au for the construction of the derivative KS operator matrix used for the response property calculation. We used the POLAR keyword in deMon2k program, which gives dipole-based polarizabilities using finite-field approximation for obtaining the values of α and β using 0.0032 au field strength for comparison with our results. The CARTESIAN option was used for the orbitals with restricted KS (RKS) scheme of calculation, where the grid accuracy of 10^{-6} au was used for the property calculations. The density convergence was set to 10^{-10} au for the DFT calculations. Our calculations have been done using the deMon2k, whereas the MP2 results[8] used for comparison are from GAMESS[40] and using a field strength of 0.001 au Davis et al.[8] have halved the hyperpolarizability values from the GAMESS program when reporting. We therefore use a factor of 2 for the hyperpolarizability values from ref 8for convenience in comparison with our results. It can be noted that the calculated average static first hyperpolarizability, β values are comparable to the experimental quantity, $\beta(-2\omega;\omega,\omega)$, obtained from the solution-phase electric field induced second-harmonic generation (EFISH) experiments. [7]

Results and Discussion

The DFT dipole moments, mean polarizability, polarizability anisotropy, and orientationally averaged polarizability and first hyperpolarizabilities at the BP86, BPW91, and BLYP level using the deMon2k are presented in Tables 1− 8. The finite-field dipole-based calculated values of polarizability and first hyperpolarizability from deMon2k program are also given in each of the tables for comparison with the results from our method. Finally, our results are compared to the benchmark MP2 values of Davis et al.[8] obtained using the energy-based finite-field method as available in the GAMESS[40] quantum chemistry program. The optical gap or the energy difference between the highest-occupied molecular orbital (HOMO) and the lowest-unoccupied molecular orbital (LUMO), from DFT and MP2 calculations are compared. We now delve into the intricacies involved in the interpretation of our NLO property results. An important objective of the NLO property calculations of PNA and its methyl-substituted derivatives is that they provide an insight into the subtle variations reflected in the values due to change in the molecular architecture. Our results are in general agreement with those of Davis et al. [8]

We begin with discussion of the dipole moments. The dipole moment, μ, is obtained from the ground-state response of the electron density and hence does not require a density response calculation. The changes in the structure of the molecule in terms of the substituents is clearly seen from the changes in the dipole moment values in the tables, as we go from PNA to *N*-mtPNA-6 in Tables 1−8, respectively. Because of the donor amino (NH_2)

TABLE 1: Dipole Moment, Static Polarizability, First Hyperpolarizability, and Optical Gap of PNA (au.)

	FF-BP86	BP86	FF-BPW91	BPW91	FF-BLYP	BLYP	FF-MP2[a]
μ_x	3.138	3.138	3.134	3.134	3.147	3.147	2.754
μ_y	0.000	0.000	0.000	0.000	0.000	0.000	0.000
μ_z	0.000	0.000	0.000	0.000	0.000	0.000	0.000
μ	3.138	3.138	3.134	3.134	3.147	3.147	2.754
α_{xx}	166.93	166.79	166.11	165.98	168.75	168.68	148.40
α_{yy}	100.57	100.63	99.96	100.02	101.74	101.80	101.01
α_{zz}	51.07	50.97	50.41	50.31	52.24	52.20	50.95
α	106.19	106.14	105.49	105.45	107.58	107.57	100.12
$\lvert\Delta\alpha\rvert$	100.70	100.66	100.54	100.52	101.29	101.26	
β_x	653.9	634.4	643.0	636.9	660.9	661.4	668.0
β_y	−2.8	0.0	−5.8	0.0	−1.2	0.0	0.1
β_z	0.0	0.0	0.0	0.0	0.0	0.0	−0.2
β	653.9	634.4	643.0	636.9	660.9	661.4	668.0
ΔE		0.2152		0.2146		0.2100	0.3717

[a] Reference 8.

TABLE 2: Dipole Moment, Static Polarizability, First Hyperpolarizability, and Optical Gap of 2-Methyl-4-nitroaniline (PNA-2) (au.)

	FF-BP86	BP86	FF-BPW91	BPW91	FF-BLYP	BLYP	FF-MP2[a]
μ_x	3.160	3.160	3.157	3.157	3.171	3.172	2.771
μ_y	−0.204	−0.204	−0.203	−0.203	−0.200	−0.200	−0.176
μ_z	0.000	0.000	0.000	0.000	0.000	0.000	0.000
μ	3.167	3.167	3.164	3.164	3.177	3.178	2.776
α_{xx}	176.74	176.76	175.85	175.89	178.32	178.38	156.44
α_{yy}	118.57	118.58	117.87	117.88	119.72	119.76	116.89
α_{zz}	59.78	59.72	59.04	58.97	60.90	60.92	59.31
α	118.36	118.36	117.59	117.59	119.65	119.70	110.88
$\lvert\Delta\alpha\rvert$	101.68	101.74	101.55	101.64	102.06	102.10	
β_x	670.7	658.2	674.3	650.1	680.4	678.3	663.7
β_y	−29.1	−32.3	−25.1	−29.8	−27.2	−28.5	−22.5
β_z	0.0	0.0	0.0	0.0	0.0	0.0	0.3
β	671.3	659.0	674.8	650.8	680.9	678.9	664.1
ΔE		0.2081		0.2077		0.2032	0.3657

[a] Reference 8.

TABLE 3: Dipole Moment, Static Polarizability, First Hyperpolarizability, and Optical Gap of 3-Methyl-4-nitroaniline (PNA-3) (au.)

	FF-BP86	BP86	FF-BPW91	BPW91	FF-BLYP	BLYP	FF-MP2[a]
μ_x	2.956	2.955	2.952	2.952	2.968	2.968	2.630
μ_y	−0.174	−0.173	−0.174	−0.174	−0.174	−0.174	−0.139
μ_z	0.000	0.000	0.000	0.000	0.000	0.000	0.000
μ	2.961	2.961	2.957	2.957	2.973	2.973	2.633
α_{xx}	175.77	175.80	174.87	174.73	177.34	177.34	159.71
α_{yy}	118.92	118.80	118.19	117.98	119.80	119.92	116.80
α_{zz}	59.80	59.93	59.06	58.96	60.90	60.95	59.27
α	118.16	118.18	117.37	117.23	119.35	119.41	111.92
$\lvert\Delta\alpha\rvert$	100.63	100.57	100.49	100.49	101.03	101.06	
β_x	542.4	526.7	545.2	528.1	546.8	543.8	610.0
β_y	3.7	−9.4	−0.5	−6.8	−0.2	−9.4	25.0
β_z	0.0	0.0	0.0	0.0	0.0	0.0	−0.7
β	542.4	526.8	545.2	528.1	546.8	543.9	610.5
ΔE		0.2209		0.2202		0.2155	0.3760

[a] ref [8]

group substituted at the para position to the nitro (NO_2) group of the benzene ring and the orientation of the molecular skeleton, the major component of the dipole moment is along the *x* axis. It can be noted that the MP2 values of the total dipole moment as well as its components are less than the corresponding values from the DFT in all the tables irrespective of the exchange-correlation functional used, except for the *y* component of *N*-mtPNA-3 in Table 6, where the MP2 dipole moment value is higher by ∼0.02 au. In case of PNA in Table 1, the components along the *y* axis are zero. However, there is a noticeable increase in the *y* component of the dipole moment as we move to the other derivative molecules. This happens as the polarity in the molecules changes in the *y* plane of the molecule due to substitution of the methyl group to the PNA skeleton. As a result, due to the substitution of the methyl group at the ring position, the symmetry of molecule in terms of the delocalized π-electron cloud is lost. This happens due to electron donating inductive effect of the methyl group which thus leads to a small polarity along the *y* axis of the molecule. The inductive effects[41] arise due to the nonequal sharing of the bonding electrons in the σ bond. All inductive effects are permanent polarizations in the ground state of molecules and

TABLE 4: Dipole Moment, Static Polarizability, First Hyperpolarizability, and Optical Gap of *N*-Methyl-4-nitroaniline (*N*-mtPNA) (au.)

	FF-BP86	BP86	FF-BPW91	BPW91	FF-BLYP	BLYP	FF-MP2[a]
μ_x	3.356	3.356	3.353	3.352	3.366	3.367	2.95
μ_y	−0.284	−0.284	−0.282	−0.282	−0.288	−0.288	−0.272
μ_z	0.000	0.000	0.000	0.000	0.000	0.000	0.000
μ	3.368	3.368	3.365	3.364	3.378	3.379	2.963
α_{xx}	195.76	195.50	194.67	194.49	197.37	196.81	172.77
α_{yy}	111.18	110.91	110.52	110.17	112.42	112.02	110.93
α_{zz}	60.57	60.49	59.80	59.72	61.70	61.68	60.06
α	122.50	122.32	121.66	121.48	123.83	123.52	114.59
$\|\Delta\alpha\|$	118.31	118.21	117.99	117.98	118.73	118.36	
β_x	837.6	837.7	830.2	838.6	860.2	854.2	851.9
β_y	−56.2	−47.2	−51.6	−45.8	−31.6	−50.3	−51.7
β_z	0.0	0.0	0.2	0.0	0.3	0.1	2.0
β	839.5	839.0	831.8	839.9	860.8	855.7	853.5
ΔE		0.0935		0.1977		0.1933	0.3652

[a] Reference 8.

TABLE 5: Dipole Moment, Static Polarizability, First Hyperpolarizability, and Optical Gap of *N*-Methyl-2-methyl-4-nitroaniline (*N*-mtPNA-2) (au.)

	FF-BP86	BP86	FF-BPW91	BPW91	FF-BLYP	BLYP	FF-MP2[a]
μ_x	3.506	3.506	3.502	3.503	3.522	3.522	3.097
μ_y	−0.169	−0.169	−0.168	−0.168	−0.173	−0.173	−0.167
μ_z	0.000	0.000	0.000	0.000	0.000	0.000	0.000
μ	3.510	3.510	3.506	3.507	3.526	3.526	3.101
α_{xx}	205.11	205.08	204.09	203.96	206.66	206.73	179.84
α_{yy}	127.47	127.41	126.64	126.60	128.50	128.41	125.45
α_{zz}	67.59	67.57	66.80	66.87	68.61	68.60	66.80
α	133.39	133.37	132.51	132.49	134.59	134.59	124.03
$\|\Delta\alpha\|$	119.53	119.59	119.32	119.20	120.00	120.12	
β_x	828.7	837.0	823.2	835.3	836.0	861.4	820.2
β_y	5.6	−3.2	−17.4	−5.2	−6.0	38.8	−24.3
β_z	0.0	0.0	0.1	0.0	0.0	0.0	3.5
β	828.7	837.0	823.4	835.3	836.0	862.3	820.7
ΔE		0.1882		0.1885		0.1842	0.3585

[a] ref [8]

TABLE 6: Dipole Moment, Static Polarizability, First Hyperpolarizability, and Optical Gap of *N*-Methyl-3-methyl-4-nitroaniline (*N*-mtPNA-3) (au.)

	FF-BP86	BP86	FF-BPW91	BPW91	FF-BLYP	BLYP	FF-MP2[a]
μ_x	3.185	3.185	3.182	3.182	3.199	3.200	2.842
μ_y	−0.103	−0.104	−0.101	−0.101	−0.107	−0.107	−0.127
μ_z	0.0	0.0	0.0	0.0	0.0	0.0	0.0
μ	3.187	3.187	3.184	3.184	3.201	3.201	2.845
α_{xx}	203.65	203.41	202.64	202.37	205.1	205.21	183.82
α_{yy}	129.25	129.02	128.36	128.16	130.41	130.16	126.71
α_{zz}	69.24	69.25	68.37	68.39	70.27	70.31	68.26
α	134.04	133.90	133.13	132.98	135.26	135.24	126.27
$\|\Delta\alpha\|$	116.74	116.56	116.61	116.39	117.12	117.22	
β_x	682.0	703.1	679.9	704.6	723.8	722.2	778.0
β_y	−43.5	−40.1	−45.0	−40.2	−28.0	−44.6	−31.0
β_z	0.1	0.1	0.0	0.1	0.3	0.1	1.9
β	683.4	704.2	681.4	705.7	724.3	723.6	778.6
ΔE		0.2041		0.0965		0.1995	0.3711

[a] Reference 8.

are therefore reflected in the physical properties, like the dipole moment. In case of the polarizability or the linear response coefficients,α, the MP2 values of mean polarizability as well as the components along the three directions given in the tables are, in general, less than the DFT values from our method as well as the finite-field DFT values. The values of the components of α in all the tables differ from the finite-field DFT values by not more than 1 au. The MP2 results for the components of the polarizability are, in general, less than the corresponding DFT values. This difference is more in case of the α_{xx} component in all the tables, which, in turn, is reflected by the mean polarizability values of all the molecules in Tables 1−8. The MP2 values of $\bar{\alpha}$ differ from the DFT values by at most 10 au. Among the DFT functionals used, the BLYP shows a higher value for the dipole moment as well as the mean polarizability as compared to the other two functionals, whereas, the values from the BP86 and the BPW91 functionals are closer to each other. The polarizability anisotropy values in each of the tables are comparable to each other differing at most by 1 au. The major contribution to the total β for the molecules comes from

TABLE 7: Dipole Moment, Static Polarizability, First Hyperpolarizability, and Optical Gap of *N*-Methyl-5-methyl-4-nitroaniline (*N*-mtPNA-5) (au.)

	FF-BP86	BP86	FF-BPW91	BPW91	FF-BLYP	BLYP	FF-MP2[a]
μ_x	3.146	3.146	3.143	3.143	3.161	3.161	2.807
μ_y	−0.431	−0.431	−0.431	−0.431	−0.436	−0.436	−0.391
μ_z	0.0	0.0	0.0	0.0	0.0	0.0	0.0
μ	3.175	3.175	3.172	3.172	3.191	3.191	2.834
α_{xx}	205.05	204.13	203.84	203.82	206.41	205.81	184.69
α_{yy}	128.73	128.62	127.89	127.75	129.83	129.75	126.31
α_{zz}	69.22	69.22	68.31	68.31	70.25	70.29	68.29
α	134.34	134.01	133.35	133.31	135.49	135.30	126.43
$\lvert\Delta\alpha\rvert$	118.31	117.53	118.06	118.05	118.59	118.04	
β_x	700.0	699.3	717.8	714.4	717.6	720.4	789.1
β_y	−35.8	−46.9	−40.8	−43.9	−43.8	−47.8	−72.0
β_z	0.0	1.4	0.4	0.1	0.1	0.1	0.2
β	700.9	700.9	718.9	715.7	718.9	721.9	792.4
ΔE		0.2027		0.0957		0.1980	0.3684

[a] Reference 8.

TABLE 8: Dipole Moment, Static Polarizability, First Hyperpolarizability, and Optical Gap of *N*-Methyl-6-methyl-4-nitroaniline (*N*-mtPNA-6) (au.)

	FF-BP86	BP86	FF-BPW91	BPW91	FF-BLYP	BLYP	FF-MP2[a]
μ_x	3.345	3.343	3.343	3.342	3.359	3.359	2.941
μ_y	−0.498	−0.498	−0.496	−0.496	−0.498	−0.498	−0.454
μ_z	0.0	0.0	0.0	0.0	0.0	0.0	0.0
μ	3.382	3.380	3.380	3.379	3.396	3.396	2.976
α_{xx}	204.03	203.90	203.06	202.89	205.60	205.60	179.64
α_{yy}	130.58	130.41	129.74	129.57	131.69	131.60	128.07
α_{zz}	69.16	69.11	68.26	68.37	70.17	70.21	68.24
α	134.59	134.49	133.69	133.62	135.82	135.82	125.32
$\lvert\Delta\alpha\rvert$	117.07	117.04	117.01	116.80	117.56	117.60	
β_x	817.6	838.1	814.6	837.7	839.9	862.6	841.5
β_y	−87.7	−85.6	−93.9	−81.5	−85.8	−83.9	−81.0
β_z	0.1	0.1	0.1	0.1	0.1	0.1	2.9
β	822.3	842.5	820.0	841.7	844.3	866.7	845.4
ΔE		0.1916		0.1918		0.2912	0.3598

[a] Reference 8.

the β_x component. The DFT values of orientationally averaged β and the total β values in each table are, in general, comparable to each other as well as to the MP2 values for the respective molecule. When studying the connection of chemical structure with the second-order nonlinear response coefficients, β, we note the second-order NLO effects in the organic molecules due to the strong donor−acceptor kind of intramolecular interaction. Also, the magnitude of the coefficient β is relatively larger than the α values of PNA and its derivatives, which is due to the highly asymmetric charge distribution in the molecules. The NH_2 group is an electron donating (ortho- and meta-directing) group, whereas the NO_2 group is an electron-withdrawing (meta-directing) group. This implies that the donor−acceptor kind of moieties at opposite ends in the PNA skeleton leads to intramolecular charge transfer. It is well known that molecules with π-conjugation and that have this kind of donor−acceptor arrangement show higher NLO responses, which is a result of the delocalization of the π electron cloud over the molecule. The donor π conjugate-bridge-acceptor forms a typical SHG-active molecule, if it lacks center of symmetry. However, the presence of the donor−acceptor in a molecule alone does not guarantee the NLO effects. Also, the molecule will not show NLO effects if the molecule possesses a center of symmetry. In PNA, the presence of a desirable resonance structure, in addition to the intramolecular charge transfer, leads to the high value of β. However, the crystalline form of PNA has a centrosymmetric structure that does not show any macroscopic second-order NLO response. We have, therefore, considered the methyl-substituted derivatives of PNA here, which eliminates the center of symmetry in the molecule thus leading to noncentrosymmetric crystal structure. The substitution of a methyl group to the benzene ring brings in asymmetry to a high degree in the electronic distribution which is reflected in the β values of the derivatives. In the case of PNA-2, where the CH_3 group is at the ortho position to the NH_2, the β values show an increase from the PNA, whereas the optical gap shows a decrease. Interestingly, for the PNA-3 with the CH_3 group at the meta position, there is an noticeable decrease in the β value and increase in the optical gap from that of PNA. The behavior of both ΔE and β for PNA-2 and PNA-3 can be explained as follows. Here, the molecular orbital picture also plays a crucial role in deciding the extent of charge transfer in terms of the HOMO−LUMO gap or the optical gap,[2] which, in turn, can be used to understand its effect on the β values. ΔE is directly proportional to the extent of charge transfer. For a small optical gap, the charge transfer occurs easily, thus, giving a higher value of β. The source of charge transfer is thus controlled by the energy of the HOMO, whereas the acceptance of the charge is dominated by the LUMO energy. Although quantitatively smaller, the methyl group shows an electron-donating inductive effect. In PNA-2, the methyl substitution is at the carbon closer to the electron-donating group, which leads to a higher HOMO energy and a lower LUMO energy, as compared to PNA-3. This leads to a smaller HOMO−LUMO energy gap for PNA-2 as compared to PNA-3. This small optical gap enhances further the charge transfer, which, in turn, is reflected in the larger

values of β for PNA-2 than PNA-3. The trends in optical gap from our method matches with that shown by MP2 method. The decrease in the optical gap leading to increase in the NLO responses allows both α and β to be more clearly illustrated, when we substitute the amine H in PNA by a methyl group in *N*-mtPNA. This relation of the optical gap with β and other higher-order response coefficients could be used to tailor NLO materials, to obtain materials with increased optical responses, by manipulating the optical gap using variable molecular substituents. The optical gap values for the *N*-mtPNA and its derivatives can also be interpreted using a similar argument. By further study of the *N*-mtPNA and its methyl-substituted derivatives, we find that the 2- and 6-methyl-substituted *N*-mtPNA derivatives show the above-mentioned correlation of the HOMO−LUMO energy gap by a distinct increase in β values. However, the change in the α values for the above molecules is not very clearly visible. Alternatively, the *N*-mtPNA-3 and *N*-mtPNA-5 with the methyl substitution at the ortho position to the NO_2 meta-directing group shows a decrease in the β values from *N*-mtPNA as the inductive effect of the methyl substituent is suppressed at this particular position. This, in turn, also quenches the polarization in the molecule, which is reflected in the dipole moment values of *N*-mtPNA-3 and *N* mtPNA-5, which are less than the parent *N*-mtPNA. The *N*-mtPNA dipole moment shows an increase from the parent PNA on methyl substitution at the amine position. Also, we find that the substitution at the N position gives higher α and β values in comparison to the isoelectronic counterparts of *N*-mtPNA, i.e., PNA-2 and PNA-3. The substitution of a second methyl to *N*-mtPNA at different positions can, thus, give us insight into the chemistry involved, which can be useful in designing materials with increased NLO responses.

Conclusion and Scope

In this paper we have studied dipole moments, static polarizability and first hyperpolarizability using our noniterative numerical-analytic density functional response method. We found that the noniterative approximation of CPKS method yielded reasonably good values of polarizability as well as first hyperpolarizability for the π-conjugated donor−acceptor organic derivatives of PNA and its methyl-substituted analogs. In the case of PNA and its derivatives, our calculations could reproduce the trends observed by Davis et al.[8] Optical gap is directly proportional to extent of charge transfer, the smaller the optical gap, easier the charge transfer and higher the β value. The trend in optical gap from our method matches with that shown by MP2 method. The effect of substitution on the NLO responses of the molecule and its effect on the optical gap were highlighted. The effect of position of substitution on β and dipole moment values were also discussed. This study could be further extended to include substitutions using different organic fragments and the solvent effects, which are missing in the present study and could be the subject of future study. The results for the calculations using noniterative CPKS is computationally effective and thus can be exploited for enhancing the applicability of the DFT for calculation of the response properties for large systems employing large basis sets.

Acknowledgment. S.P. acknowledges partial financial assistance from SSB and a J.C.Bose fellowship grant towards fulfillment of this work.

References and Notes

(1) Chemla, D.; Zyss, S. J. *Nonlinear Optical Properties of Organic Molecules and crystals*; Academic Press: New York, 1987; Vol. 1.

(2) Kanis, D. R.; Ratner, M. A.; Marks, T. J. *Chem. Rev.* **1994**, *94*, 195.

(3) Champagne, B.; Kirtman, B. *Handbook of Advanced Electronic and Photonic Materials*; Nalwa, H. S., Ed.; Academic, San Diego, 2001; Vol *9*, Chapter 2, p 63.

(4) Morley, J. *J. Phys. Chem.* **1994**, *98*, 11818.

(5) Bishop, D. M. *Adv. Chem. Phys.* **1998**, *104*, 1.

(6) Sim, F.; Chin, S.; Dupuis, M.; Rice, J. E. *J. Phys. Chem.* **1993**, *97*, 1158.

(7) Daniel, C.; Dupuis, M. *Chem. Phys. Lett.* **1990**, *171*, 209.

(8) Davis, D.; Sreekumar, K.; Sajeev, Y.; Pal, S. *J. Phys. Chem. B* **2005**, *109*, 14093.

(9) Ågren, H.; Vahtras, O.; Koch, H.; Jørgensen, P. *J. Chem. Phys.* **1993**, *98*, 6417.

(10) Mikkelsen, K. V.; Luo, Y.; Ågren, H.; Jørgensen, P. *J. Chem. Phys.* **1994**, *102*, 9362.

(11) Champagne, B.; Perpete, E. A.; Jacquemin, D.; van Gisbergen, S. J. A.; Baerends, E. -J.; Soubra-Ghaoui, C.; Robins, K. A.; Kirtman, B. *J. Phys. Chem. A* **2000**, *104*, 4755.

(12) Champagne, B. *Chem. Phys. Lett.* **1996**, *261*, 57.

(13) Quinet, O.; Champagne, B.; Kirtman, B. *J. Mol. Struct.* **2003**, *633*, 199.

(14) Bulat, F.; Toro-Labbé, A.; Champagne, B.; Kirtman, B.; Yang, W. *J. Chem. Phys.* **2005**, *123*, 14319.

(15) Sekino, H.; Bartlett, R. J. *J. Chem. Phys.* **1986**, *84*, 2726.

(16) Kondo, A. E.; Piecuch, P.; Paldus, J. *J. Chem. Phys.* **1996**, *104*, 8566.

(17) Sekino, H.; Bartlett, R. J. *J. Chem. Phys.* **1993**, *98*, 3022.

(18) Ghose, K. B.; Piecuch, P.; Pal, S.; Adamowicz, L. *J. Chem. Phys.* **1996**, *104*, 6582.

(19) Bishop, D. M.; Pipin, J.; Lam, B. *Chem. Phys. Lett.* **1986**, *127*, 377.

(20) Ingamells, V. E.; Papadopoulos, M. G.; Handy, N. C.; Willetts, A. *J. Chem. Phys.* **1998**, *109*, 1845.

(21) Salter, E. A.; Sekino, H.; Bartlett, R. J. *J. Chem. Phys.* **1987**, *87*, 502.

(22) Bartlett, R. J.; Purvis, G. D. *Phys. Rev. A* **1979**, *20*, 1313.

(23) Guan, J.; Duffy, P.; Carter, J. T.; Chong, D. P.; Casida, K. C.; Casida, M. E.; Wrinn, M. *J. Chem. Phys.* **1993**, *98*, 4753.

(24) Kobayashi, R.; Koch, H.; Jorgenson, P.; Lee, T. J. *Chem. Phys. Lett.* **1993**, *211*, 94.

(25) Sophy, K. B. PhD Thesis, University of Pune, India, 2007.

(26) Sophy, K. B.; Pal, S. *J. Chem. Phys.* **2003**, *118*, 10861.

(27) Sophy, K. B.; Pal, S. *J. Mol. Struct. THEOCHEM* **2004**, *676*, 89.

(28) Pal, S.; Sophy, K. B. In *Lecture Series on Computer and Computational Sciences 3*; Brill Academic Publishers, Netherlands, 2005; p 142.

(29) Sophy, K. B.; Calaminici, P.; Pal, S. *J. Chem. Theory Comput.* **2007**, *3*, 716.

(30) Dykstra, C. E; Jasien, P. G. *Chem. Phys. Lett.* **1984**, *109*, 388.

(31) Epstein, S. T. *The Variation Method in Quantum Chemistry*; Academic Press, New York, 1974.

(32) Hellmann, H. *Einführung in die Quantenchemie*; Deuticke, Leipzig, 1937, p 285.

(33) Feynman, R. P. *Phys. Rev.* **1939**, *56*, 340.

(34) Pulay, P. J. *J. Chem. Phys.* **1983**, *78*, 5043.

(35) Köster, A. M.; Calaminici, P.; Flores, R.; Geudtner, G.; Goursot, A.; Heine, T.; Janetzko, F.; Patchkovskii, S.; Reveles, J. U.; Vela, A.; Salahub, D. R. *deMon2k*, The deMon developers, Cinvestav, 2004.

(36) Becke, A. D. *Phys. Rev. A* **1988**, *38*, 3098.

(37) Perdew, J. P. *Phys. Rev. B* **1986**, *33*, 8822.

(38) Perdew, J. P.; Wang, Y. *Phys. Rev. B* **1992**, *45*, 13244.

(39) Lee, C.; Yang, W.; Parr, R. G. *Phys. Rev. B* **1988**, *37*, 785.

(40) Schmidt, M. W.; Baldridge, K. K.; Boatz, J. A.; Elbert, S. T.; Gordon, M. S.; Jensen, J. H.; Koseki, S.; Matsunaga, N.; Nguyen, K. A.; Su, S. J.; Windus, T. L.; Dupius, M.; Montgomery, J. A. J. *Comput. Chem.* **1993**, *14*, 1347.

(41) Sykes, P. *A guide book to mechanism in inorganic chemistry*; Orient Longman: New Delhi, 1986.

JP806204Q